

Neutron/gamma pulse shape discrimination in EJ-299-34 at high flux

Christopher Payne, Paul J. Sellin, Mark Ellis, Kirk Duroe, George Randall, Robert Speller, Ashley Jones, Malcolm Joyce, Member, IEEE

Abstract— The effect of scintillator geometry on the quality of neutron/ γ pulse shape discrimination (PSD) in EJ-299 plastic scintillator, using a digital charge integration PSD algorithm has been studied. It is shown that the PSD Figure of Merit (FOM) reduces as the geometry of the scintillator moves from a cube-like shape towards a flat panel shape. The PSD performance in this material at high flux irradiation is investigated with performance deteriorating at rates of $\sim 10^7$ photons/s. The use of EJ-299 for security applications, with a focus on active interrogation environments is explored in conjunction with a system capable of neutron/ γ separation and localisation.

I. INTRODUCTION

IN this paper the high flux n/ γ PSD performance of Eljen EJ-299-34 plastic scintillator is studied. This work is in the context of security applications, with a focus on active interrogation, for n/ γ detection in which the n/ γ separation achieved by the scintillator may be potentially degraded in very intense dynamic radiation fields. This study of PSD in EJ-299-34 builds on the original reports of PSD in this material by Lawrence Livermore Laboratories, and other groups, in which n/ γ discrimination was reported with good PSD performance across the full energy range [1]. Recently the n/ γ PSD Figure of Merit (FOM) of EJ-299 variants has been characterised in a range of commercial and bespoke detectors, see for example [2]. The FOM reported for EJ-299-34 are generally worse than for conventional liquid scintillators such as BC-501A; at 1 MeV the FOM for BC-501A was seen in our own work to be double that of EJ-299-34. However, the performance is more than adequate for a range of potential applications. In the security field the ability to use a plastic scintillator with good PSD performance is extremely attractive due to it being nontoxic unlike older liquid scintillators, having greater stability at varying temperatures, controlled geometry and can be easily machined into desired geometries.

C.Payne and P.Sellin are with the Department of Physics, University of Surrey, UK.

M.Ellis and K.Duroe are with AWE, Reading, UK.

G.Randall and R.Speller are with the Department of Medical Physics and Biomedical Engineering, University College London

A.Jones and M.Joyce are with the Department of Engineering, University of Lancaster, UK

This work is supported by the U.K. Home Office and Ministry of Defence.

Manuscript received November ##, 2015; revised November 23, 2015.

©British Crown Owned Copyright 2015/AWE

Active interrogation is a technique, currently being investigated by AWE [3-4], to detect special nuclear material (SNM). An external source of radiation is used to induce fission within the SNM, the products of which can be detected to indicate its presence [5]. Experiments have been conducted with systems which produce a high intensity initial radiation “flash”, that lasts on the order of 10-100 nanoseconds. In these experiments [6-7] detectors typically become saturated and unresponsive for milliseconds after the probe pulse. This “dead time” overlaps with the delayed radiation from induced fission and therefore information about the fission events is lost by the time the detectors have recovered.

The aim of this work is to produce a detector system capable of operating in this environment. Due to the dynamic nature of the radiation environment the detector must become active when the radiation from the initial pulse reduces to levels low enough for it to function correctly; information for this is provided by a second, more robust, detector system. The detector must also perform rudimentary imaging (localization) and achieve n/ γ discrimination. To achieve this EJ-299-34 has been evaluated for use in conjunction with a redesign of the ‘RadICAL’ system [8] previously created at UCL to form a static n/ γ imaging system. Using the RadICAL concept, the shape of the EJ-299-34 scintillator elements must be long and thin in order to provide localization information. As this geometry tends to degrade PSD performance compromises must therefore be made in order to achieve usable levels of both PSD and localisation.

This paper focuses on two aspects of EJ-299-34 performance; the optimisation of PSD performance for large aspect-ratio pieces of EJ-299-34 scintillator, up to 125 x 25 x 15mm, and the assessment of the PSD performance under high incident radiation rates. Commercial EJ-299-33 detectors are currently available only in a range of cylindrical scintillator geometries. In this project we are working with thin rectangular slabs of scintillator, which show significantly different PSD properties compared to cylindrical pieces.

II. METHODS

A. Digital PSD performance

The PSD performance of EJ-299-34 in a range of geometries has been tested. For each geometry the EJ-299-34 was cut and polished to the desired dimensions and coupled to a fast ETL 9102B photomultiplier tube (PMT) within a light-tight enclosure. The PSD performance of geometries between

15x15x15mm and 125 x 25 x 15mm have been tested for gamma and neutron events from 100 keVee to approximately 4 MeVee using an Am/Be source. Samples were polished manually to optical standards and then encapsulated in titanium oxide paint to aid the light collection.

Energy spectra and PSD measurements were taken using a mixed n/γ field produced from an Am/Be source contained in a water tank. An air pipe was inserted into the water tank to displace the water and expose the detector to a fast neutron beam. The Am/Be source also produces a gamma field that originates from the source itself and from the neutron interactions with the moderating water. Energy calibrations were carried out using Compton edge energies from gamma sources - as the scintillator is a low Z material no photo peaks are present in the detector's pulse height spectrum.

The PSD studies have been carried out using a variety of CAEN waveform digitisers (Table 1). Each pulse was analysed in real time using the CAEN digital pulse processor (DPP) to extract the integrated charge, and PSD parameter for each event. The CAEN digital pulse shape algorithm was used to obtain the PSD parameter, which is a digital version of the standard two-gate charge integrator algorithm, where the PSD parameter is given by [9]:

$$PSD = \frac{Q_{long} - Q_{short}}{Q_{long}} \quad (1)$$

Where Q_{short} is the charge contained in the short gate and Q_{long} the charge in the entire pulse. Both gates are measured from the same time and so the difference, $Q_{long} - Q_{short}$, yields the charge in the tail of the pulse which is then normalised by the total charge. As neutron pulses exhibit a greater proportion of charge in the tail of the pulse compared to gammas, Figure 1, equation 1 results in neutrons having larger PSD values than gamma events. Optimal PSD performance was obtained with a 52ns short gate and a 320ns long gate.

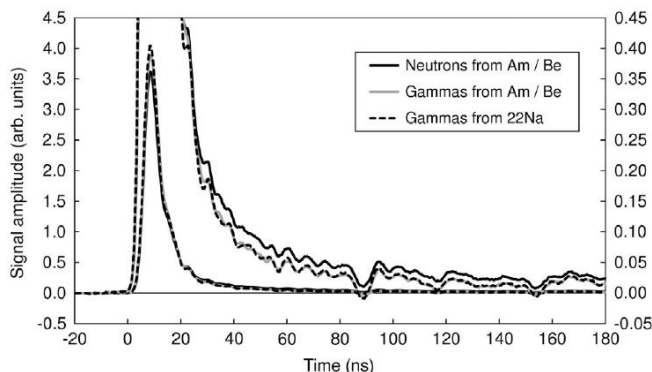


Fig1: Average measured pulse shapes for neutrons and gammas. Each shape is plotted twice, once showing the entire trace and again at a magnification factor of 10 (see right-hand scale) so as to show the pulse tail in detail [10].

The CAEN DPP-PSD software is capable of outputting list-mode data files. For each triggered event the output contains the timestamp, the charge in the short and long gates, and the

PSD value calculated using equation 1. The resulting event file was analysed offline using a MatLab script to generate event-by-event energy spectra and 2D plots of PSD vs Energy, and to carry out the FOM analysis of the n/γ separation as a function of energy.

The conventional figure of merit (FOM) value is calculated as shown in Figure 2. This is the standard metric used to define a detector's PSD performance, in which a FOM greater than 1.27 corresponds to separated Gaussian distributions and therefore a high level of PSD capability [1]. In the FOM equation shown in Figure 2, W_a and W_b are the full width half maxima (FWHM) of the two distributions, assumed Gaussian, whilst X is the separation between the distribution means. For this work FOM values are calculated of all events above the given energy threshold, i.e. a FOM for an energy of 1 MeV will have been calculated using events of 1 MeV and greater.

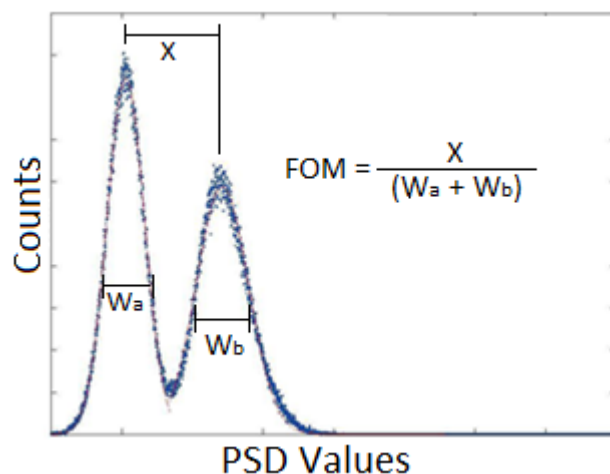


Fig 2: Example PSD spectra with the calculation of the Figure of Merit, in this case W_a represents gamma events whilst W_b neutrons.

High levels of PSD performance is challenging in EJ-299-34 since the respective neutron and gamma pulse shapes differ only slightly due to small differences in the ratio of the short/long decay time constants, see Figure 1 [10]. The three CAEN digitisers used in this study provide a range of digital sampling rates and ADC resolutions (Table 1). Figure 3 shows the resulting FOM functions for the 3 digitisers, as a function of threshold energy. We conclude that the higher 14-bit resolution of the DT5730 performs best for this material, despite a slightly slower sampling rate of 500 MS/s. The PSD FOM values achieved with the DT5730 were on average 18% better than for the V1751 for 1 MeVee events. However, due to equipment availability, the majority of this work was carried out using the CAEN V1751 digitizer which, although exhibiting a lower ADC resolution than the DT5730, still provides sufficient PSD performance for our purposes.

Digitizer	ADC bit resolution	Sample Rate	Analogue range V _{pp}	Channels
V1751	10	1 GS/s	1	8
V1720	12	250 MS/s	2	8
DT5730	14	500 MS/s	2	8

Table 1: List of Digitisers that have been used in this project

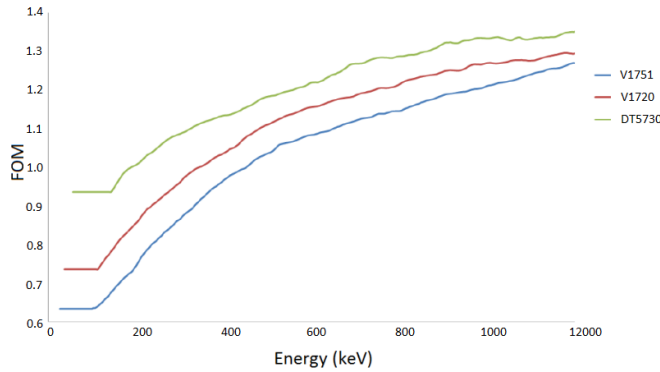


Fig 3: FOM as a function of threshold energy for a 25x25x15mm piece of EJ-299-34 scintillator, measured with three different CAEN digitisers.

B. High Flux Studies

The potential degradation of PSD performance in EJ-299-34 as a function of event rate has been investigated. It is anticipated that pile-up effects in the detector will eventually cause the digital PSD algorithm to break down as the event rate is increased to very high values. To investigate this effect, we have used an EJ-299-33 detector supplied by Scionix with an electronic gating circuit incorporated within the PMT. Application of the gating signal allows the detector to be inhibited during very high flux conditions. To achieve gating, the detector is supplied with an external 5V DC signal, when the gate signal is low the PMT becomes active. In the final design a Si Pin Diode will control this signal, turning off when the background level radiation is low enough for the PMT in the scintillator detector to function correctly. The performance of this detector has been studied using a miniature Amptek X-ray tube to saturate the detector with low energy (40 kV max) photons, whilst the detector simultaneously acquires gamma pulses from a ^{22}Na source. A rotating lead collimator containing a narrow slot was placed between the X-ray tube and the detector, as shown in Figure 4. When the slot is momentarily aligned in front of the detector, the intense photon flux is incident on the EJ-299-34 scintillator, and the detector is saturated. The edge of the lead slot has a graded thickness, so as the slot rotates past the detector the incident photon flux gradually reduces to zero. By varying the delay time of the gating circuit, the PSD performance of the detector is sampled as it acquires ^{22}Na events as a function of incident photon flux.

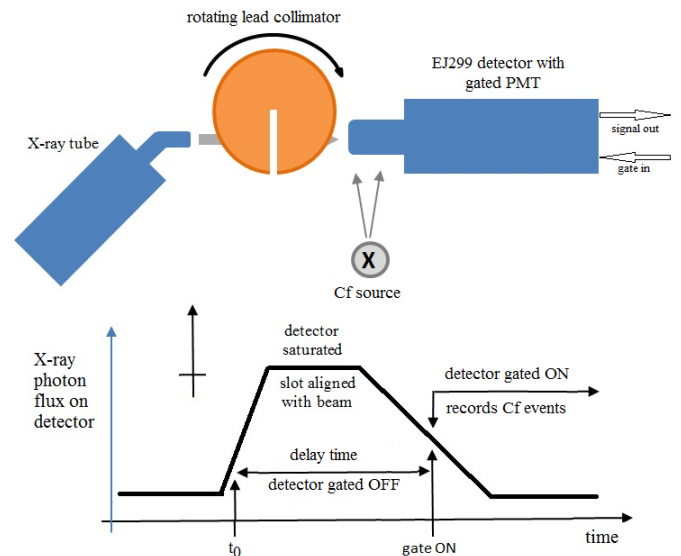


Figure 4. Schematic of the high flux irradiation system showing the ideal setup where a Cf source has been used instead of only a gamma emitting source

III. RESULTS

The n/γ performances for a range of cuboid pieces of EJ-299-34 have been studied, using the real-time CAEN digital PSD algorithm. A typical 2D plot of PSD vs Energy is shown in Figure 5, which shows n/γ separation for a piece of EJ-299-34 measuring 25x25x15mm. Figure 5 also shows the energy dependence of the PSD FOM for various shaped scintillators. The PSD performance generally improves with energy, reaching a FOM of 1.4 for a 25x25x15mm scintillator at photon energy of 1 MeV. The data also shows a general trend of reduced FOM when moving from a cube to a flat sheet. Improvements to the PSD performance can be achieved by improving the light collection and hence the signal/noise ratio, and by optimising the optical path and reflective surfaces of the scintillator element. The use of Perspex light guides was studied to see if they improved PSD performance, however no measurable improvement was observed.

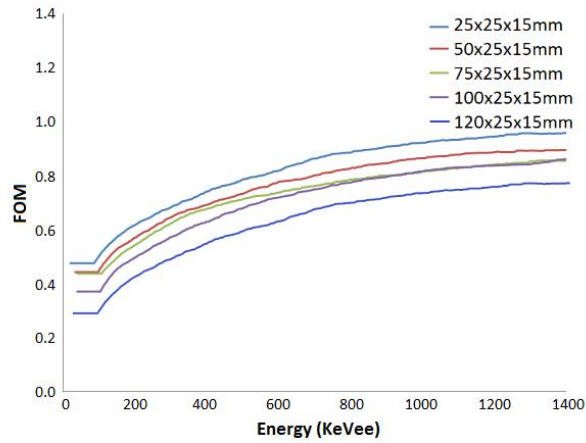
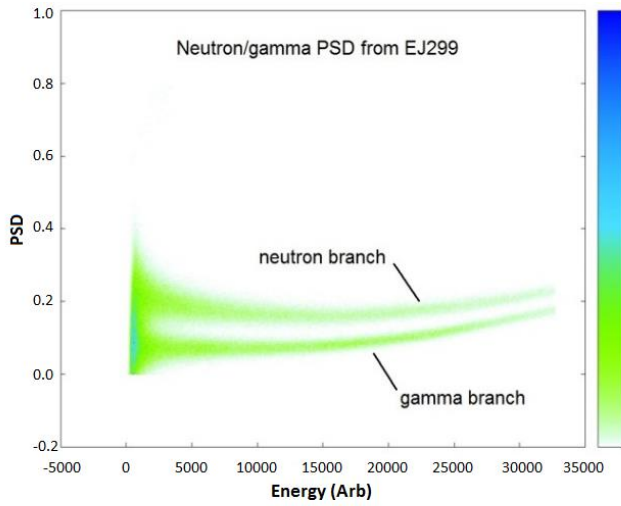


Fig. 5. (top) 2D plot, for a 25x25x15mm piece of EJ-299-34, of PSD against energy for an Am/Be mixed n/ γ flux, (bottom) PSD FOM as a function of photon energy for a range of EJ-299-34 scintillator geometries

To measure the high flux rate PSD performance of the scintillator the X-ray tube was used to irradiate the detector whilst simultaneously acquiring source data. Initially this study only used gamma events from a ^{22}Na source. Figure 6 shows 2D plots of the gamma events from ^{22}Na recorded by EJ-299-34, shown (top) without X-ray irradiation, and (bottom) with an X-ray flux of approximately 3×10^7 photons/s incident onto the detector. The gamma data shown in Figure 6 clearly shows the degradation in PSD performance, broader gamma distribution, of the scintillator in the presence of $\sim 10^7$ photons/sec of low energy X-rays. This effect could be due to pile-up effects at high count rate that tend to degrade the performance of the digital PSD algorithm, or it could come from more complex optical effects in the scintillator due to optical saturation at high event rate.

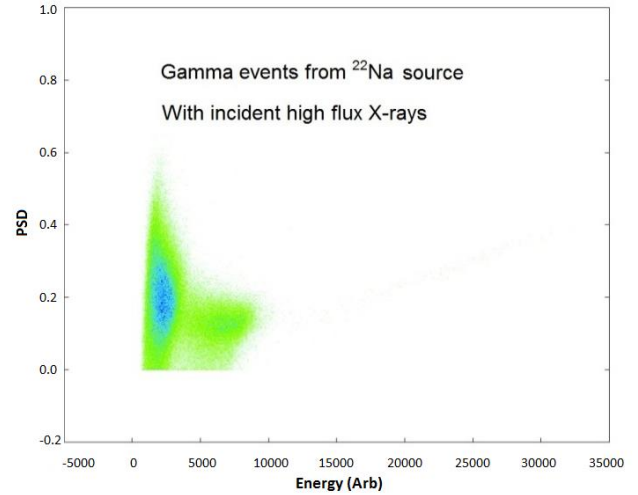
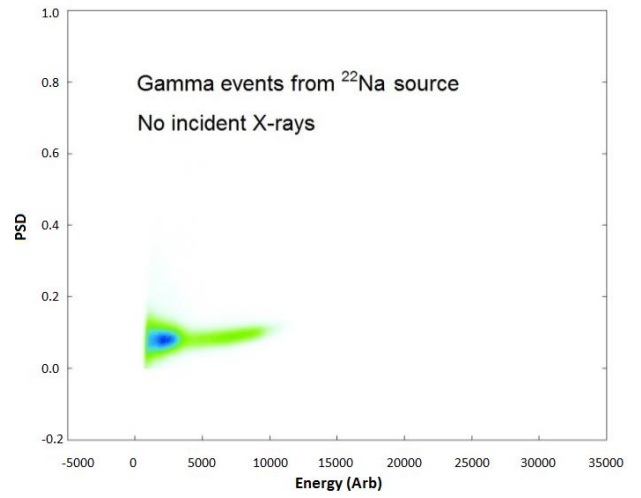


Figure 6: 2D plots of PSD vs energy for gamma events from ^{22}Na . (top) without X-ray irradiation, (bottom) with simultaneous high flux X-ray irradiation.

IV. CONCLUSION

This work characterises the PSD performance of EJ-299-34 scintillator for a range of operating conditions that are appropriate for some security applications, with a focus on active interrogation. This includes a study of the PSD performance for scintillator pieces that are cuboid in shape; this shape is required by the proposed method of source localisation. The trend shows that as one dimension of the scintillator increases, whilst holding the other two sides fixed, the PSD performance degrades. The FOM for a 120x25x15mm piece for 1 MeVee events is 20% worse than the 25x25x15mm piece.

Our study shows that the signal to noise ratio in the detected pulses is a key factor that affects PSD performance. We have also shown that this can be optimised through the correct choice of high ADC resolution digitiser. We have studied how PSD performance is affected at high flux, and using a 'chopped beam' from a laboratory X-ray tube the degradation in PSD performance at high photon flux has been demonstrated.

REFERENCES

- [1] N. Zaitseva, B. L. Rupert, I. Paweczak, A. Glenn, H. P. Martinez, L. Carman, M. Faust, N. Cherepy, and S. Payne, *NIM A* 668 (2012) 88–93.
- [2] S.A. Pozzi, M.M. Bourne, S.D. Clarke, *NIM A* 723 (2013) 19-23.
- [3] C. Hill, J. O'Malley, P. N. Martin, K. Marshall, R. Maddock, J. Threadgold, R. Comisso, S. L. Jackson, J. Schumer, B. Philps, P. Ottinger, D. Mosher, J. Apruzese, F. Young, and J. Davis, "Active Detection of Special Nuclear Material Recommendations for Interrogation Source Approach for UK Prototype Active Detection System," 2012.
- [4] C. D. Clemett, M. Ellis, C. Hill, J. Threadgold, P. N. Martin, S. L. Jackson, J. C. Zier, D. D. Hinshelwood, L. Mitchell, R. Woolf, and D. Mosher, "Neutrons for Active Detection of Special Nuclear Material: an Intense Pulsed $^7\text{Li}(p,n)^7\text{Be}$ Source," 2012.
- [5] M. Gmar, E. Berthoumieux, S. Boyer, F. Carrel, D. Dor, M.-L. Giacri, F. Lain, B. Poumarde, D. Ridikas, and A. Van Lauwe, "Detection of nuclear material by photon activation inside cargo containers," *Non-Intrusive Inspection Technologies, Proceedings of SPIE*, vol. 6213, p. 62130F, 2006.
- [6] C. Hill, J. O'Malley, M. Ellis, P. Mistry, R. Maddock, J. Precious, J. C. Zier, S. L. Jackson, A. Hutcheson, L. Mitchell, and B. Philps, "Photofission for Active SNM Detection I: Intense Pulsed 8MeV Bremsstrahlung Source," 2012.
- [7] P. Mistry, C. Hill, J. O'Malley, J. Precious, M. Ellis, R. Maddock, F. C. Young, S. L. Jackson, D. G. Phipps, R. Woolf, and B. Philps, "Photofission for Active SNM Detection: Intense Pulsed $^{19}\text{F}(p,\alpha,\gamma)^{16}\text{O}$ Characteristic gamma Source," 2012.
- [8] G. L. Randall, E. Iglesias, H. F. Wong, and R. S. Speller, *J. Instrum.* 9 (2014) 10011.
- [9] <http://www.caen.it> DPP – PSD Control Software
- [10] N. Hawkes and G. Taylor, *NIM A* 729 (2013) 522–526.